3rd International Symposium on
Connections between Steel and Concrete
Stuttgart, Germany, September 27th -29th , 2017

INFLUENCE OF EDGE BEARING ON THE FRONT-EDGE SHEAR BREAKOUT CAPACITY

Neal S. Anderson[1*] and Donald F. Meinheit[2]
[1]Simpson, Gumpertz and Heger, Chicago, Illinois, USA
[2]Wiss, Janney, Elstner Associates, Inc., Chicago, Illinois, USA
*Corresponding Author Email: nsanderson@sgh.com

ABSTRACT

Edge bearing stresses on shear-loaded anchorages can enhance the shear capacity because of the confining stresses provided by the compressive bearing stress. However, too much bearing stress can have a negative influence on the shear breakout strength; the higher bearing stress cracks the concrete in a pattern similar to the failure from a pure bearing load, compromising the shear breakout when the anchorage is near an edge. A pilot test program of 11 tests was conducted to examine this effect; this work was initiated from an investigation of a precast wall panel anchorage failure (gravity and wind connection), where the bearing stress on an embedded anchorage likely reduced the concrete shear breakout capacity when the anchorage was near the free edge of the concrete member.

The ACI 318-14 Building Code, Chapter 17 recognizes the interaction of tension and shear on a connection, yet the interaction between bearing (compression) and shear does not appear to have ever been studied experimentally. This pilot test program examined plain steel plates (plates resting on the top of the concrete with a thin layer of grout beneath the plate) loaded in compression and plates with headed studs embedded in concrete loaded in compression with the compression load near an edge. The test specimens were not limited by any lateral side boundary conditions. This paper examines the second phase of testing where headed-stud connections were loaded toward a free edge with an orthogonally applied edge-bearing load. Bearing stress ranged from 0 to 16.4 MPa (2,375 psi) and the front-edge distance to the studs ranged from 51 to 76 mm (2 to 3 in.). One edge of the anchorage plate in bearing was located flush with the edge of the concrete. Concrete cover requirements were maintained on the embedded anchors.

The test findings showed that the shear capacity of the embedded anchorage increased as the bearing stress increased. However, above a bearing stress of 17.2 MPa (2,500 psi), the influence of bearing stress was adverse and reduced the shear breakout capacity computed by ACI 318 methods. A modification relationship to account for this affect is proposed.

1 Introduction

In investigating the cause of a precast concrete panel falling off a hotel facade in the Midwest United States, we uncovered an interesting behavior of the panel connection. The panel-to-structure connection, shown in Figures 1 and 2, applied the panel gravity load to a spandrel beam. The connection consisted of an angle bearing on a steel plate, attached to the top horizontal surface of a

spandrel beam, with expansion or post-installed concrete anchors. The anchors were installed at a point atop the spandrel beam, outside the reinforcement cage core. Our investigation of the connection shear capacity revealed a reduced shear capacity due to the gravity load bearing on the connection plate attached to the spandrel.

Other conditions like the one shown in Figures 1 and 2 exist when precast elements bear on supporting members. Two simple examples are the precast tee stems bearing on a ledger beam, Figure 3, and an inverted-tee beam or a stem of a precast tee beam bearing on a corbel, as sketched in Figure 4. In each of these conditions, the connection has a shear force applied toward a free edge due to time-dependent shrinkage or temperature deformations.

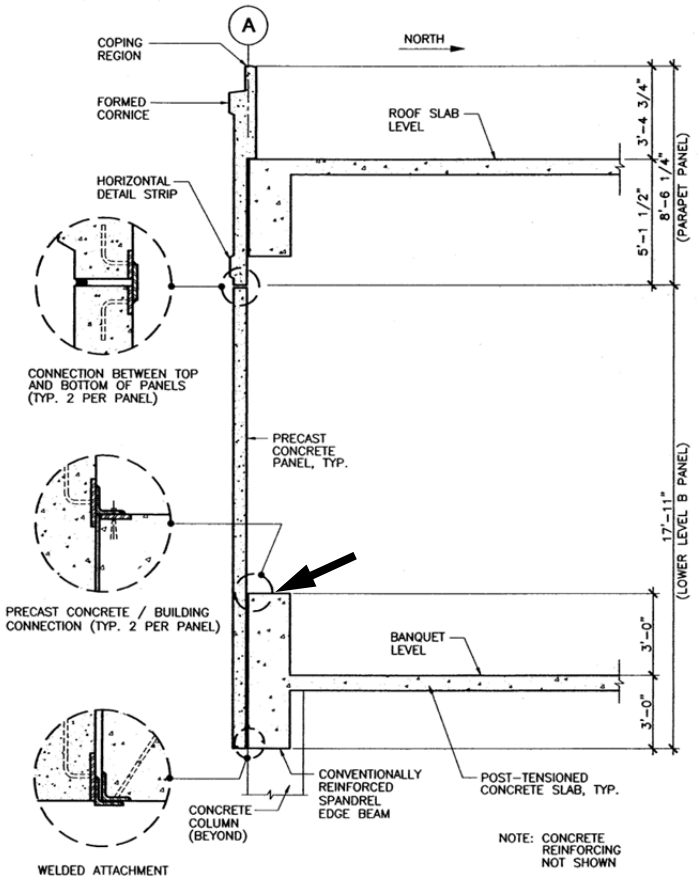

Figure 1: Cross section of cladding panel supported by a spandrel beam

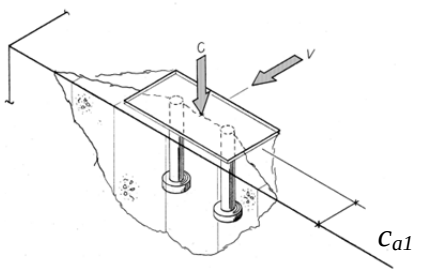

Figure 2: Loads on embedded anchorages in top of spandrel; see middle connection in Figure 1. (C = Compression or bearing force, V = Shear)

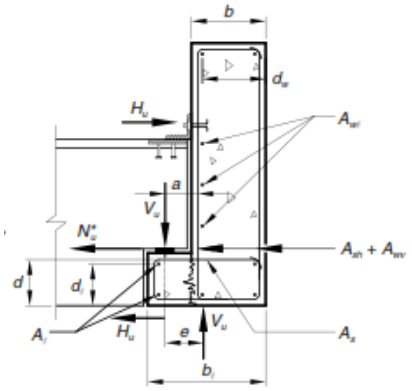

Figure 3 – Typical ledger beam supporting stems of precast double-tee members.

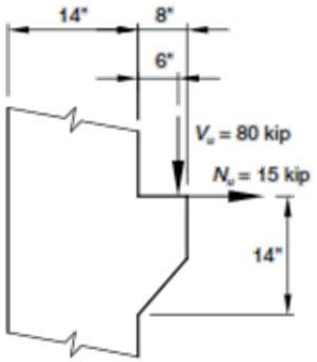

Figure 4 – Typical loading on a column corbel from an inverted-tee beam or precast double-tee beam stem (1 in. = 25.4 mm, 1 kip = 4.448 kN)

2 Past Research

In 1963, Kriz and Raths investigated the bearing strength of column heads at the Portland Cement Association (PCA) Laboratories[1]. Their testing resulted in a bearing strength relationship for finite-width column heads, which can be found as Equation 5-54 in the PCI Handbook - 7th Edition[2]. The PCA investigators noted that "the bearing strength of column heads is reduced considerably when outward horizontal forces (N_u) are applied in combination with the vertical loads." This conclusion can be carried over to the shear strength of a headed stud anchorages near an edge if affected by a concentrated compressive force. As shown in the PCI equation below, Equation 1 (English Units), it is difficult to determine the shear strength of a headed stud connection if written in this form. V_n is the vertical bearing strength, V_u is the bearing load and N_u is normal to the vertical load, that is, the shear load. In addition, the PCA research did not use headed studs to anchor the column head bearing plate. The steel bearing only rested on the column head concrete.

$$\phi V_n = \phi \left(\frac{sw}{200}\right)^{\frac{N_u}{V_u}} (0.85 f_c' A_1) \sqrt{\frac{A_2}{A_1}} \leq 1.1 f_c' A_1 \quad (1)$$

Based on the hotel facade investigation and 1963 PCA research, we believe a combined compression-shear interaction relationship exists when concrete anchors are located within 3 to 5 anchor diameters from a concrete edge; this represents a front-edge distance within the side concrete cover. The edge distance represented in the PCA equation is an arbitrary distance whereby any lateral reinforcement in the member would be ineffective. The PCA testing focused on the bearing capacity, V_n, of a precast concrete column head. This paper inverts the focus and examines the shear strength of a headed-stud connection under the presence of an axial compressive load. Moreover, no lateral side edges will be present to limit the transverse width of the concrete breakout surface. The testing reported herein applies to any bearing seat anchored by headed studs.

3 Experimental Program

An experimental program was performed where a shear-loaded anchorage located close to an edge was subject to combined shear and bearing loads. A previous pilot testing program with bearing-only loads was conducted prior to this testing. We found the edge-bearing capacity of concrete is quite high, with bearing loads about 10 times greater than the predicted shear load. Thus, we selected realistic, in-service bearing stresses for these test anchorages, and theorized the bearing influence on shear capacity would be a multiplicative factor, instead of an interaction relationship.

3.1 Test Specimens

The anchorages were located at the edge of a 1.5 x 3.0 x 0.4 m (5 ft x 10 ft x 1 ft-3 in.) deep concrete specimen used for pryout testing for another experimental study. Tests were conducted by restraining the movement of the specimen. The simple loading apparatus and test slab is shown in Figure 5.

Front-edge distance to the headed studs was 51 or 76 mm (2 or 3 in.), and the, s_1, anchor spacing was either 89 or 114 mm (3.5 or 4.5 in.). All tests used a two-stud anchorage configuration in the near-edge location. Headed studs were 12.7 mm (1/2 in.) in diameter with an effective depth, h_{ef}, of 81 mm (3.2 in.). The h_{ef} / d_a ratio was a constant 6.4. The ultimate tensile strength of the headed studs was 536 MPa (77.7 ksi). All load-deformation curves for the headed studs tested in direct tension in air exhibited rounded, but ductile, behavior. Steel failures did not govern any of the testing reported herein.

The steel plates used were 12.7 mm (1/2 in.) thick. Plate sizes are shown in Table 1 with a calculated bearing contact area of 15,490 or 20,650 sq. mm (24 or 32 sq. in.). The right-hand column of Table 1 shows the three plate configurations used. The plates had extensions that projected beyond the slab edge. As shown, the plate extension had a hole for a bolt and clevis assembly for the shear-load application.

Table 1 – Steel plate dimensions for the anchorage tests

(1)	(2)	(3)	(4)	(5)	(6)	
Test Plate	Test Geometry		Brg Plate Size		Bearing Area (mm^2)	
	c_{a1} (mm)	s_1 (mm)	x (mm)	y (mm)		
PL-7A	50.8	88.9	152.4	101.6	15485	
PL-7B	76.2	88.9	152.4	101.6	15485	
PL-8A	50.8	114.3	203.2	101.6	20645	
Plate thickness = 12.7 mm, ASTM A36 plate						1 in. = 25.4 mm

All edge plates were positioned on the form bottom so 0.4 m (1 ft - 3 in.) of concrete was placed above. This ensured good consolidation around the headed studs and thus trapped air voids beneath the bearing plate were eliminated. The slabs were reinforced with a nominal amount of welded wire reinforcement (WWR) for handling purposes; where applicable, the mesh was cut away in the

vicinity of the stud anchorages to avoid any possible contribution of reinforcement to the measured test load.

3.2 Concrete Properties

The concrete slab was cast with a nominal 41.5 MPa (6,000 psi) normal weight concrete mixture containing 12.7 mm (1/2 in.) angular, granite gravel, and no air entrainment. The concrete properties are presented in Table 2 for the tests. We started testing the anchorages at a concrete age of 23 days and finished at 45 days. Concrete cylinder compressive strengths were obtained at the beginning and end of testing, and at 28 days. The static modulus of elasticity was tested at the same time as the concrete compressive strength. Tensile split-cylinder tests were also performed at the beginning and end of testing. The tensile strengths obtained were consistent with values expected. The concrete strength was not a variable in the experimental program.

Table 2 – Concrete properties for the tests

(1)	(2)	(3)	(4)	(5)	(6)
Concrete Age (days)	Average Values (150 x 300 mm cylinders)				Notes
	f'_c (MPa)	Static Modulus, E (MPa)	Tensile Strength f_{sp} (MPa)	n	
14	37.2	-	-		
23	40.3	28,020	3.3	0.53	Start testing
28	40.8	29,070			
45	43.4	28,730	4.0	0.61	Finish testing
Average		28,610			
Notes: Col (2) Col (5)	Compressive strength based on the average of three (3), 150 x 300 mm cylinders. where $f_{sp} = n\,(f'_c)^{0.5}$ Concrete unit weight = 2,420 kg / cubic meter (normal weight)				
SI Units:	1,000 psi = 6.895 MPa, 1 pcf = 16.026 kg / cubic meter				

3.3 Test Procedures

Figure 5 shows the test set-up. Each slab was tested flat, and the slab was rotated in-plane to access other embedded edge anchorages located on the sides. A test frame was built above the slab and tied down to the test floor for the bearing reaction. The shear test frame reacted near the ends of the slab edge, as to be located outside the potential breakout cone that forms along the long-edge direction of the test specimen. Test loads were applied with a manually operated hydraulic ram and loads were measured with a load cell. Displacement instrumentation, was measured continuously during the test to failure. After the failure, the characteristics of all concrete breakout surfaces were documented.

Test bearing load levels were selected as $0.0f'_c$ (pure shear), $0.1f'_c$, $0.2f'_c$, $0.3f'_c$, and $0.4f'_c$. For most tests, the bearing load was held constant and the shear load was applied. For two tests, the bearing load was linearly increased simultaneously with the shear load. To assure full bearing on the plate, a sheet of greased Teflon® (PTFE) was placed on the bearing surface and a “wedding cake” of thick steel plates was stacked to gradually spread the bearing load. For all tests, the shear load was increased until failure occurred.

Figure 5 – Overall view of the test set-up showing both bearing and shear load application.

4 Test Results

Table 3 presents the test results, along with the actual measured values of the geometry and material properties. Due to concrete shear breakout surfaces being larger than anticipated, two test anchorages were damaged, with their breakout cones truncated. Observations of the failure surfaces follow:

Low Bearing Stress – These tests involve those with targeted bearing stress levels of $0.0f'_c$ (pure shear), $0.1f'_c$ and $0.2f'_c$. The two, pure shear tests were typical shear breakout surfaces and served as calibration tests. For tests with target bearing levels of $0.1f'_c$ and $0.2f'_c$, the shear capacity developed was greater than the no bearing load condition. Figure 6 shows the breakout with a nominal bearing stress of $0.1f'_c$. The concrete breakout surface was deeper and the entire shaft length (depth) of the stud was exposed; the entire stud length formed part of the final failure surface. (*Note in all the photographs, the stud head impression in the concrete was colored with a* ***black*** *marker, post-test, for reference.*) Instead of the top one or two diameters of the stud bearing on the concrete, it appeared the compressive confinement of the bearing load activated more stud length in resisting the shear force.

Figure 7 shows two test breakouts where the bearing stress was $0.2f'_c$. Again the breakout was deeper and had a vertical back face. In addition, the breakout started to activate a second crack front propagating at the rear of the plate. This is illustrated better in Figure 8, looking down at the breakout. Again, the shear capacity of the anchorage exceeded both the test sets with $0.0f'_c$ (pure shear) and $0.1f'_c$ bearing levels.

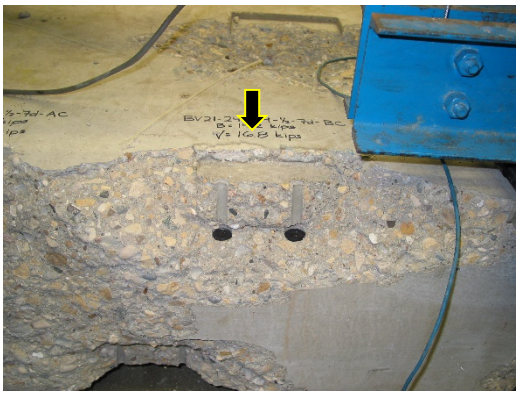

Figure 6 – Test BV21-24-6.4-1/2-7d-BC with a bearing stress of $0.1f'_c$.

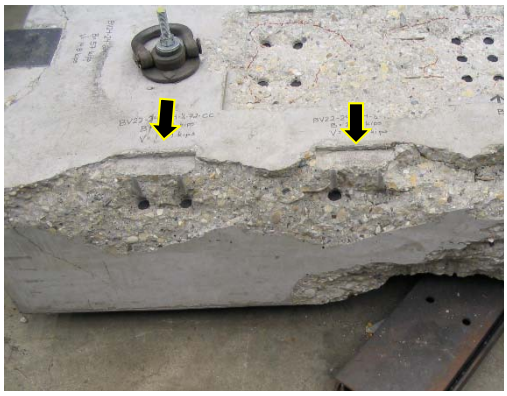

Figure 7 – Overall view of two shear tests with a $0.2f'_c$ bearing stress.

High Bearing Stress – These tests involve targeted bearing stress levels of $0.3f'_c$, and $0.4f'_c$. The measured shear capacity of the anchorage exceeded that of the pure shear case, but the shear capacity increase measured in the $0.1f_c'$ and $0.2f_c'$ tests seemed to diminished. The shear strength appeared to peak between the $0.2f'_c$ and $0.3f'_c$ bearing load.

Figure 8 – Test BV22-24-6.4-1/2-7d-CC with a bearing stress of $0.2f'_c$.

Figure 9 – Test BV24-24-6.4-1/2-7d-BCN with a bearing stress of $0.4f'_c$.

Figure 9 illustrates the failure crack at ultimate load with a $0.4f'_c$ bearing stress. Note the crack propagation around the back edge of the plate. The higher bearing load activated a failure surface more representative of a bearing-type failure; the whole plate area was a contributor.

Figure 10 is a similar situation for a target $0.3f'_c$ bearing stress level. The failure crack propagated around the back edge of the plate (Figure 10(a)), and resulted in a fairly large shear breakout cone. Upon removal of the concrete piece in Figure 10(b), the failure surface revealed a sharp, vertical face corresponding to the rear crack face. The entire stud anchorage was buried in the breakout piece and the studs did not contribute to forming the breakout crack surface. The vertical face was approximately the depth of the headed studs. Edge bearing of the concrete seemed to be the dominant action.

(a) Breakout showing the development of the rear crack behind the anchor plate. The studs are contained in the breakout concrete.

(b) Breakout concrete removed showing the vertical rear crack surface to a depth lower than the studs. The studs did not intersect the crack failure surface.

Figure 10 – Test BV21-24-6.4-1/2-7d-BC with a bearing stress of $0.3f'_c$.

Bearing Load Application – Tests BV22-24-6.4-1/2-7d-AC and BV22-24-6.4-1/2-7d-CC are compared to BV22-24-6.4-1/2-7d-AL and BV22-24-6.4-1/2-7d-BL in this section. The former two tests used a constantly applied bearing load, whereas the latter two tests had the bearing load increasing during the test. No conclusions can be drawn from the two test sets as the failure loads were consistent. Although the goal was to increase the bearing load linearly, the load application became more of a step loading on account of the manual hand pump used for the ram.

5 Data Analysis

The shear load capacity is predicted given two methods. The first method is the PCI Design Handbook[2] method formulated by the authors[3]. This method was derived from extensive experimental testing of headed stud anchorages. The second analysis method is the concrete capacity design (CCD) method from Chapter 17 of ACI 318-14[4,5].

Figure 11 shows the experimental behavior expressed as the test-to-predicted capacity versus the bearing stress referenced to the actual concrete compressive strength. The shear capacity was predicted with the average PCI shear equation using the PCI spacing factor for the two-stud pattern. The figure implies a beneficial effect of the bearing load on the connection up to f_{brg} / f_c' of about 0.42. For bearing stress levels, f_{brg} / f_c' of 0.1 to 0.3, the anchorage shear capacity increased and in some instances doubled (2x). As we observed during the testing, the peak effect seemed to occur around $f_{brg} / f_c' = 0.2$. Above that level of bearing stress, the improved shear strength diminished as the bearing behavior governed at the higher bearing load(s).

The average concrete capacity design (CCD) shear prediction from Chapter 17 of ACI 318-14 is shown in Figure 12. The data trend of the plot is similar, but generally shifted upward for the headed studs. This demonstrates the CCD method is conservative when the edge distance is small (51 or 76 mm) and the spacing influence for the two-stud group is factored into the strength calculation for this close edge distance.

The influence of bearing on a shear-loaded anchorage is complicated, given the curvilinear nature of the relationship. A bearing load on the anchorage helps, but the benefits disappear when the bearing level is approximately 40 percent of the concrete compressive strength. We performed no tests above this 40 percent bearing level, so we recommend an upper limit on the influence. Given the nature of curtain wall or facade gravity loadings at an edge, this upper bound limit seems reasonable for this connection.

The failure surfaces at the higher bearing levels ($0.3f'_c$, and $0.4f'_c$) were revealing with respect to behavior. At high bearing stress, the shear load seems to disrupt the edge bearing mechanism. At high bearing stress levels, the bearing mechanism is more dominant than the near-edge shear resistance. This behavior was evidenced by the rear boundary of the breakout surface being defined at the edge of the bearing plate. Moreover, the rear crack face was near-vertical before turning outward to the slab edge.

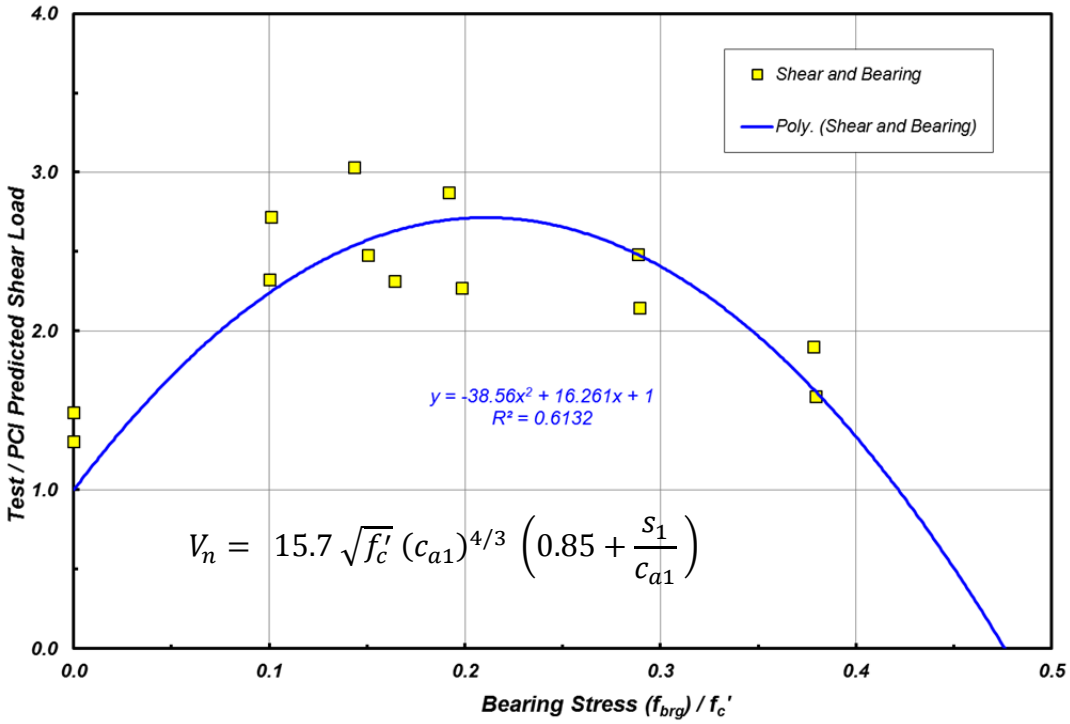

Figure 11 – Test-to-predicted (average) shear failure load (PCI) versus the bearing stress level expressed as a function of the concrete compressive strength.

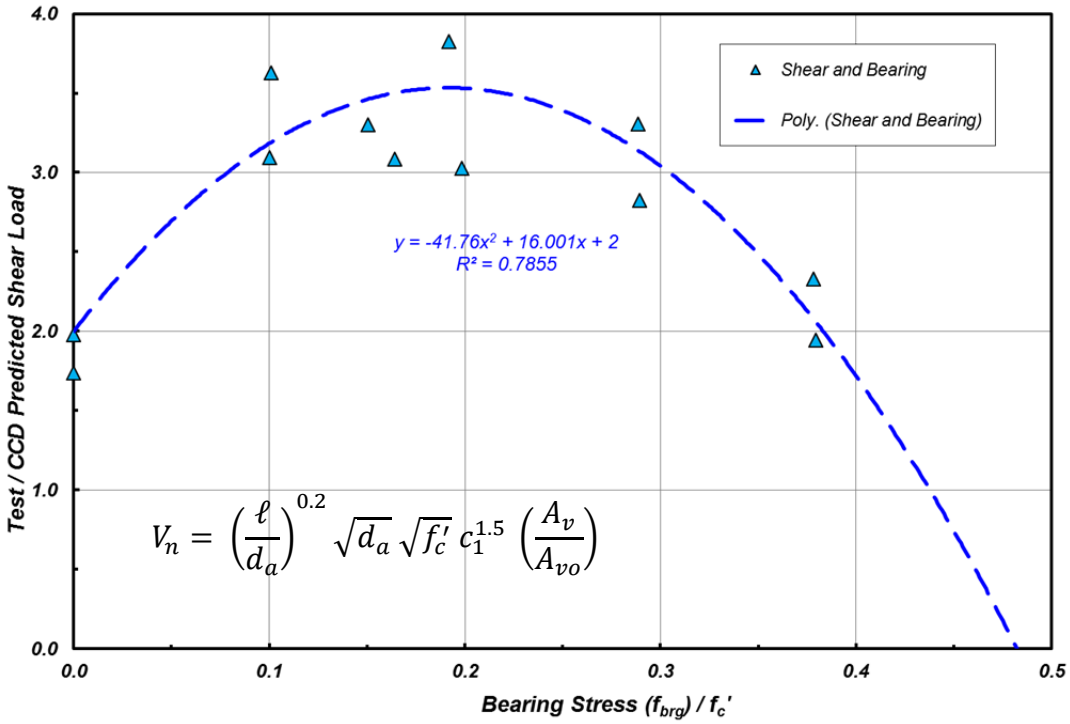

Figure 12 – Test-to-predicted (average) shear failure load (ACI-CCD) versus the bearing stress level expressed as a function of the concrete compressive strength.

The data presented a non-intuitive challenge to defining the bearing influence on a shear-loaded anchorage near an edge. The data can be fit to a curved, polynomial relationship, and the challenge was to simplify the bearing-shear interaction computation. We considered a tri-linear interaction curve, but viewed it to be too complicated. Additionally, we briefly studied the behavior of compressive-loaded shear lugs and there may be a correlation in the factors proposed in the literature.

Because the bearing influence on an anchorage will likely occur very near a front-edge, we selected the PCI Handbook equation as the basis for our analysis. Consequently, the selected modification factor for compressive bearing would be conservative for the CCD predictor. Given the two-stud anchorages of this test program, the best-fit relationship is shown in the plot of Figure 11; for the 13 tests, the correlation coefficient, R-squared, is 0.61. To provide a polynomial factor that passes through 1.0, a bearing effect modification factor for a shear-loaded anchorage is proposed as Equation 2:

$$\psi_{brg,V} = 17\eta(1 - 2.4\eta) + 1 \quad (2)$$

$$\text{where: } \eta = \frac{f_{brg}}{f_c'} \text{ and } 0 \leq \eta \leq 0.42$$

The maximum bearing stress level is limited to 0.42 in this factor. This represents the present limitation of this research. In addition, bearing levels this high on a near-edge shear anchorage no longer appear to be an anchorage-to-concrete capacity determination; the behavior appears to be dominated by bearing. If the bearing stress is zero, the factor reduces to 1.0.

6 Conclusion

Additional research is recommended beyond these 11 multiple-anchor tests with combined bearing and shear to refine a bearing influence factor. The behavior was observed to change as the bearing stress was increased. At low bearing stress, less than about $0.2f_c'$, the breakout crack propagated through the line of headed stud anchors. Above about $0.3f_c'$, the breakout initiated at the rear of the plate and did not propagate through the stud anchors. The breakout crack also took on a new unique shape, propagating vertically to the depth of the anchor and then proceeding outward to the free edge of the concrete.

Bearing stress on an embed plate can have a beneficial effect but that benefit appears to be limited by a bearing stress near $0.4f_c'$. Scatter exists in the 11 test samples reported. However, a reasonably simple bearing stress modifier is proposed for designing when combinations of bearing and shear exist simultaneously.

7 Acknowledgement

The authors wish to express their appreciation to the Wiss, Janney, Elstner Associates, Inc. (WJE) for the use of their testing equipment and portions of concrete specimens to cast these anchorages into a concrete slab. The authors would also like to thank the contributions of Messrs. Harry Chambers, Don Sues, and Don Mercker of Nelson Stud Welding for their donation of headed studs and stud welding services. Thanks also to Mr. Roger Becker, who at the time the testing was

conducted was Vice President of Spancrete Industries, for Spancrete's casting of the test samples. The authors are also indebted the Precast/Prestressed Concrete Institute for initially sponsoring and extensive research project, which had a few leftover anchorage plates and headed studs because the test program scope changed as information on the shear behavior of welded headed stud anchors became available.

References

1. Kriz, L.B. and Raths, C.H. (1963), “Connections in Precast Concrete Structures – Bearing Strength of Column Heads”, Bulletin D73, Development Department, Portland Cement Association, Skokie, Illinois, USA, December, 30 pp.

2. Precast / Prestressed Concrete Institute (2010), PCI Design Handbook, 7th Edition, (PCI MNL 120-10), Precast / Prestressed Concrete Institute, Chicago, Illinois, USA.

3. Anderson, N.S. and Meinheit, D.F. (2007), “A Review of the Chapter 6 Headed Stud Design Criteria in the 6th Edition PCI Handbook”, PCI Journal, Vol. 52, No. 1, January/February, pp 84-115.

4. ACI Committee 318 (2014), Building Code Requirements for Structural Concrete (ACI 318-14), and Commentary on Building Code Requirements for Structural Concrete (ACI 318R-14) American Concrete Institute, Farmington Hills, MI, 524 pp.

5. Fuchs, W., Eligehausen, R., and Breen, J.E. (1995), “Concrete Capacity Design (CCD) Approach for Fastening to Concrete”, ACI Structural Journal, Vol. 92, No. 1, January-February, pp. 73-94.

Table 3 – Test results for the combined shear and bearing tests.

(1)	(2)	(3)	(4)	(5)	(6)	(7)	(8)	(9)	(10)	(11)	(12)	(13)
Test Identification	Concrete Strength f'_c (MPa)	Test Plate	Test Geometry c_{a1} (mm)	Test Geometry s_1 (mm)	Bearing Area (mm^2)	Bearing Load B (kN)	Failure Load V (kN)	Bearing Stress, f_{brg} (MPa)	f_{brg} / f'_c	Failure Mode	PCI Test / Predicted	CCD Test / Predicted
V23-2-7-BA	40.3	7A	51	89	15485	0.0	40.2	-	-	Conc.	1.49	1.98
V23-2-7-BB	42.2	7A	51	89	15485	0.0	36.0	-	-	Conc.	1.30	1.74
BV21-24-6.4-1/2-7d-AC	40.8	7A	51	89	15485	63.2	63.2	4.1	0.10	Conc.	2.32	3.09
BV21-24-6.4-1/2-7d-BC	40.5	7A	51	92	15485	63.2	74.7	4.1	0.10	Conc.	2.72	3.63
BV215-32-6.4-1/2-9d-AC	43.3	8A	51	114	20645	128.1	94.7	6.2	0.14	Conc.	3.03	4.08
BV22-24-6.4-1/2-7d-AC	40.8	7A	51	89	15485	125.4	61.8	8.1	0.20	Conc.	2.27	3.03
BV22-24-6.4-1/2-7d-CC	42.2	7A	51	89	15485	125.4	79.4	8.1	0.19	Conc.	2.87	3.83
BV22-24-6.4-1/2-7d-AL	42.2	7A	51	89	15485	107.2	64.1	6.9	0.16	Conc.	2.32	3.08
BV22-24-6.4-1/2-7d-BL	42.2	7A	51	89	15485	98.3	68.5	6.3	0.15	Conc.	2.48	3.30
BV23-24-6.4-1/2-7d-AC	42.2	7A	54	89	15485	189.0	62.9	12.2	0.29	Conc.	2.15	2.82
BV23-24-6.4-1/2-7d-CC	42.3	7A	51	89	15485	189.0	68.8	12.2	0.29	Conc.	2.48	3.31
BV24-24-6.4-1/2-7d-ACN	43.3	7B	76	89	15485	253.5	79.0	16.4	0.38	Conc.	1.90	2.33
BV24-24-6.4-1/2-7d-BCN	43.2	7B	76	89	15485	253.5	65.8	16.4	0.38	Conc.	1.59	1.95
BV23-24-6.4-1/2-7d-BC	42.2	7A	51	89	15485	189.0	43.2	12.2	0.29	Damage	1.56	2.08
BV23-32-6.4-1/2-9d-BC	43.2	8A	51	114	20645	253.5	43.6	12.3	0.28	Damage	1.40	1.88

Column (1): BV - (no. of studs) (bearing level: n x f_c') – (bearing area) - (h_{ef} /d_a ratio) – (stud diameter) - (s_2 spacing) - (A, B, C, or D test)(C=constant bearing, L=increasing bearing, N=bearing non-concentric over studs) [units: inches]
BV = Bearing –Shear
Column (10): Bearing stress expressed as a percentage of the concrete compressive strength.
Column (12 & 13): Average equations used in the analysis.

Conversions: 1 in. = 25.4 mm, 1 ksi = 6.895 MPa, 1 lb = 4.448 N, 1 kip = 4.448 kN, 1 lb/ft^3 = 16.03 kg/m^3